Angular distribution of neutrons from deuterated cluster explosions driven by femtosecond laser pulses

F. Buersgens, K. W. Madison,* D. R. Symes, R. Hartke, J. Osterhoff, W. Grigsby, G. Dyer, and T. Ditmire
The Texas Center for High Intensity Laser Science, Department of Physics, University of Texas at Austin, Austin, Texas 78712, USA
(Received 15 February 2005; revised manuscript received 5 January 2006; published 13 July 2006)

We have studied experimentally the angular distributions of fusion neutrons from plasmas of multi-keV ion temperature, created by 40 fs, multi-TW laser pulses in dense plumes of D_2 and CD_4 clusters. A slight anisotropy in the neutron emission is observed. We attribute this anisotropy to the fact that the differential cross section for DD fusion is anisotropic even at low collision energies, and this, coupled with the geometry of the gas jet target, leads to beam-target neutrons that are slightly directed. The qualitative features of this anisotropy are confirmed by Monte Carlo simulations.

DOI: 10.1103/PhysRevE.74.016403 PACS number(s): 52.50.Jm, 52.38.Ph, 52.70.Nc

I. INTRODUCTION

Recently there has been considerable interest in the exploration of plasmas created by irradiation of van der Waals bonded clusters with ultrashort, intense lasers [1–3]. In these experiments the laser pulse heats the free electrons produced via ionization and drives an energetic explosion. Intense femtosecond laser interactions with clusters of low-Z atoms, such as hydrogen or deuterium, are of particular interest as a situation can be found, even in quite large clusters (of >1000 atoms each) in which the laser electric field is strong enough to extract all of the ionized electrons from the cluster. Significant or even total removal of the electrons from the cluster can be achieved almost instantaneously with short pulses (<100 fs) at intensities $>10^{17}$ W/cm^2. Subsequently, the nanometer sized clusters undergo an almost isotropic explosion driven solely by the repulsion between the ions. This Coulomb explosion picture has been discussed in recent theoretical studies [4–6] of laser irradiation of deuterated clusters. The ion energies attained (several keV) in the laser-cluster interaction are sufficient to drive nuclear fusion between deuterons through the $D+D \rightarrow {}^3He(0.82\ MeV)+n(2.45\ MeV)$ reaction [7–10]. As the clusters explode, a hot cylindrical plasma filament is created within the laser focus with a diameter determined by the laser focal spot and a length given by the penetration depth of the laser pulse into the clustering gas [9]. Nuclear reactions can occur between energetic deuterons ejected from adjacent cluster explosions within this heated plasma filament [7–9], which we term "filament fusion." The neutrons originating from this process should show nearly isotropic emission since the individual cluster explosions are isotropic. Reactions can also occur as hot deuterons stream outward into the surrounding gas and collide with cold deuterons [10]—a process we term "beam-target fusion" since it is similar to the beam-target mechanism of neutron generation common in higher density solid target experiments [11–17] in which energetic laser-accelerated deuterons are launched into a cold bulk material. The macroscopic explosion of the cluster plasma filament is primarily radial, ejecting fast deuterons mainly orthogonal to the laser propagation direction. The beam-target neutron emission has a preferred direction along the axis of the fast deuteron motion and so is expected to exhibit some asymmetry [10].

Investigations of fusion from high density ($\approx 7\times 10^{18}$ molecules cm^{-3}) D_2 cluster jets at the Lawrence Livermore National Laboratory (LLNL) found isotropic neutron emission [8] and a subnanosecond fusion burn time [9], indicating a predominance of thermonuclear fusion in the filament. In contrast, an experiment conducted at the Laboratoire d'Optique Appliquée (LOA) [10] irradiating CD_4 clusters at a lower average density ($\approx 2\times 10^{17}$ molecules cm^{-3}) produced yields too high to be explained purely in terms of filament fusion indicating a significant number of beam-target reactions. A reduction of the neutron yield in the forward direction also supported their interpretation, although the angular data were limited.

The purpose of the present study was to conduct a more detailed measurement of the angular distribution of neutrons created in a laser-irradiated cluster plasma. Through such a study, we can ascertain the relative importance of the filament fusion and beam-target fusion contributions to the neutron yield. Measurements of neutron emission from laser-produced plasmas have previously been applied to diagnose the dynamics of fast ions, which are often difficult to measure directly [12–15,18–20]. Neutrons from high intensity interactions with deuterated solid targets are generated primarily by beam-target fusion [14–16] reactions, and their angular profile is closely related to the angular profile of the deuterons accelerated by the laser. In short scale-length high density plasmas (electron density $n_e \approx 10^{23}$ cm^{-3}) under ultraintense irradiation, deuterons are accelerated in a beam into the target, imprinting a strong anisotropy on the neutron emission [12,16]. If a preplasma exists, then the deuteron acceleration spreads into a larger angle, leading to almost isotropic neutron yields [14–16]. In long scale-length plasmas, the laser pulse can also self-focus and create a channel in the underdense preplasma ($n_e \approx 10^{21}$ cm^{-3}) as electrons are expelled through the ponderomotive force of the laser. The subsequent explosion of this channel accelerates deuterons radially outward from the laser axis, driving fusion reactions in the surrounding material [11]. This contribution should cause a weak asymmetry in the neutron yield [16].

*Present address: Department of Physics and Astronomy, University of British Columbia, Vancouver, B.C., Canada V6T1Z1.

Fusion neutrons were observed from a high density ($>10^{19}$ cm^{-3}) molecular D_2 gas jet (with no clusters present) under ultrahigh intensity ($>10^{19}$ W cm^{-2}) irradiation in Ref. [18]. The ponderomotive force of the laser pulse expelled electrons from the focal region initiating a Coulomb explosion of the deuterons. The authors measured a symmetric neutron yield from the thermonuclear reactions in the plasma filament and concluded that beam-target reactions were not significant in this case. Nuclear fusion has also been achieved by irradiating a spray of 150 nm D_2O droplets at 1×10^{19} W cm^{-2} [21]. Under such high irradiance, the droplets are highly stripped of electrons and explode isotropically like clusters. In this experiment the neutron yield was also found to be symmetric.

In this paper, we present measurements of the angular distribution of fusion neutrons ejected from exploding deuterium clusters and deuterated methane clusters. We find that there is a slight but statistically significant anisotropy in the neutron spatial distribution with a peaking of the neutron yield along the axis of laser propagation. We calculated neutron distributions via Monte Carlo particle simulations including both the plasma filament and the beam-target fusion processes. Our measured neutron distribution anisotropy is explained here by considering the shape of the plasma filament and the presence of gas around the filament. The elongated shape of the interaction and surrounding gas, coupled with isotropic ion ejection from clusters in the filament, give rise to slightly higher probability of fusion collisions for ions traveling along or against the laser propagation direction. The anisotropy arises because of the slight peaking of the differential fusion cross section for the 20–50 keV deuterons which actually contribute to the fusion (i.e. the hot ion tail in the plasma) along the ion center of mass vector [22].

II. EXPERIMENTAL SETUP

In our experiments, a dense plume of either CD_4 or D_2 clusters was produced by the expansion of the gas from a high pressure (P_0=70 bar) reservoir into a vacuum. We used a 24 mm long conical, supersonic nozzle with a 750 μm orifice and an opening angle of 10°. Both gases were precooled prior to their expansion: D_2 was cooled to about 100 K and CD_4 to approximately 270 K, with a heat exchanger connected to the gas jet valve. The resulting supersonic expansion leads to a dense plume of nanometer sized clusters. The clusters were irradiated approximately 2–3 mm underneath the nozzle by a 40 fs, 800 nm pulse provided by the THOR laser. The pulse energies were in the range of 40–300 mJ. In the D_2 experiments the laser was focused by an $f/7$ plano-convex lens; an $f/12$ spherical mirror was used in the CD_4 experiments. In both cases the peak intensity was $\approx10^{17}$ W/cm^2 when 10 TW of power was employed. The polarization of the laser could be varied by introducing a $\lambda/2$ wave plate (which limited laser energy to about 100 mJ to prevent nonlinear distortion of the pulse in the optic). The average gas density was estimated using a transverse interferometric image of a hydrogen cluster plasma filament. Operating the gas jet with hydrogen cooled to 100 K, we measured an electron density of $\approx1\times10^{19}$ cm^{-3}, corresponding to a molecular H_2 density of $\approx5\times10^{18}$ cm^{-3}. The molecular density of CD_4 can be estimated as $\approx2\times10^{18}$ cm^{-3} by comparing the temperature of the gas jet in the two cases and applying the ideal gas law. These values are in good agreement with those measured for a conical gas jet in Ref. [23], although are somewhat higher than the estimate of gas density used in Ref. [10].

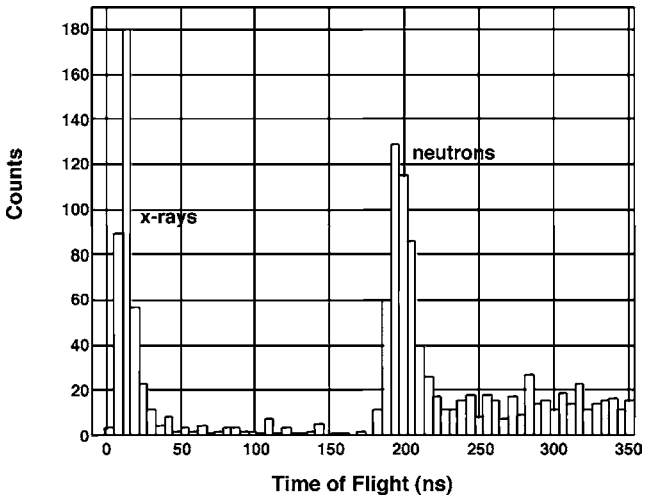

FIG. 1. Time of flight spectrum from a neutron detector placed 2.2 m from the cluster fusion plasma.

The nuclear fusion yield was monitored with a set of four neutron detectors. All detectors consisted of a scintillating plastic rod of 12.7 cm diameter and 15 cm length attached to a fast 5 in. photomultiplier tube with a conical light guide made of Plexiglas. Time of flight diagnosis permitted us to distinguish 2.45 MeV fusion neutrons from the small number of hard x-rays through the stainless steel chamber wall. Figure 1 illustrates a characteristic neutron time of flight spectrum from deuterium clusters. In the D_2 experiment, we examined yields at fixed positions and permuted the positions of all four detectors in order to account for differences in the individual sensitivities of the detectors. In the CD_4 experiment, one detector was moved and the other two detectors remained in place to use for normalization. A typical arrangement of the neutron detectors around our target chamber is illustrated in Fig. 2. Furthermore, for the CD_4 run the detectors were situated at an elevated position with respect to the gas jet (about 0.28 m, looking down at an angle of 30°–45°) in order to avoid variations in the attenuation of the neutron flux owing to different amounts of material (e.g., by flanges or windows) along the path of the neutron.

III. RESULTS

We measured angular distributions of the neutrons for both D_2 and CD_4 clusters. The experiments employing D_2 were performed at pulse energies of $\approx$200 mJ on target, which led to overall yields on the order of $\approx10^4$ fusion events per shot. The angular dependence of the neutron emission was obtained by computing the relative contribution of the detector signal from each position to the total signal of the same detector obtained by summing over all positions.

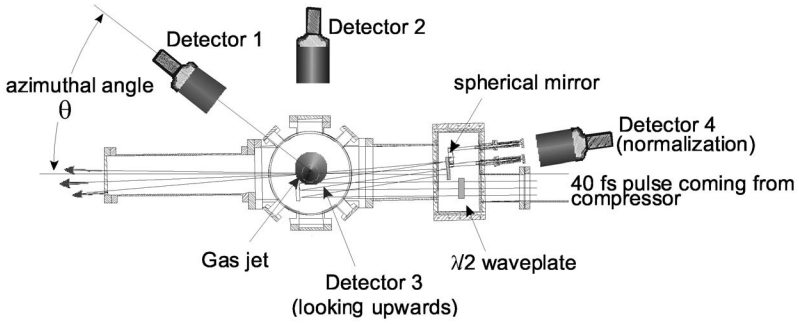

FIG. 2. Schematic of the setup used for the angular measurement of the neutron yield.

The detectors remained in each of the four positions for 250 shots. Figure 3 shows the measured neutron yield at four azimuthal angles with respect to the laser propagation direction. Each data point represents the integrated signal averaged over 1000 shots. The error bars indicate the standard deviation of the signal areas for different shots and different positions. The neutron yield is very nearly isotropic; however, it appears that a slightly decreased neutron emission probability exists for the direction perpendicular to laser propagation. Even though the size of the error bars would also be consistent with a completely isotropic neutron emission, the data are quantitatively consistent with results from a particle simulation described below.

Next, a set of experimental runs examined angular distributions of neutrons from exploding CD_4 clusters. The first experimental run in CD_4 was devoted to a measurement of the polarization dependence of the neutron emission. This measurement was motivated by the idea that all other potentially relevant physical parameters (e.g., density and cluster size distribution) can be assumed to be constant over the diameter of the plasma filament (which initially is ≤ 100 μm), such that the only preferential direction imposed in the radial direction comes from the polarization of the laser. In Fig. 4 the polarization and thus the direction of the electric field was varied by means of a $\lambda/2$ plate over a domain of approximately 0° to 160° (with 0° corresponding to **E** pointed along the detection axis). Two detectors were employed; one observing the plasma from the side (position *A*) and one directly underneath the chamber (position *B*). For each polarization, 700 shots at pulse energies of 40 mJ were averaged and the resulting average signal height was interpreted as measure for the neutron yield. It can be seen that the angular neutron yield does not vary by more than, at most, 10% for different polarizations.

Next, the azimuthal distribution of the neutron emission was measured for CD_4 clusters. In these measurements, two detectors were placed at the same, fixed position as normalization. A third detector was moved around the chamber at a slightly elevated position with respect to the gas jet. Hence the data obtained at the position of the detector were not purely azimuthal but also had a very slight polar component. This was necessary to avoid the entrance flanges on the equator of the chamber and ensure that neutrons traversed the same amount of chamber materials at every point. Neutron yield as a function of azimuthal angle for this experiment is illustrated in Fig. 5. The number of shots varies from 200 to 1800 shots per data point and results in error bars of differing length for each point. Figure 5 indicates that anisotropy exists in the neutron yield with a higher yield in the forward and backward directions.

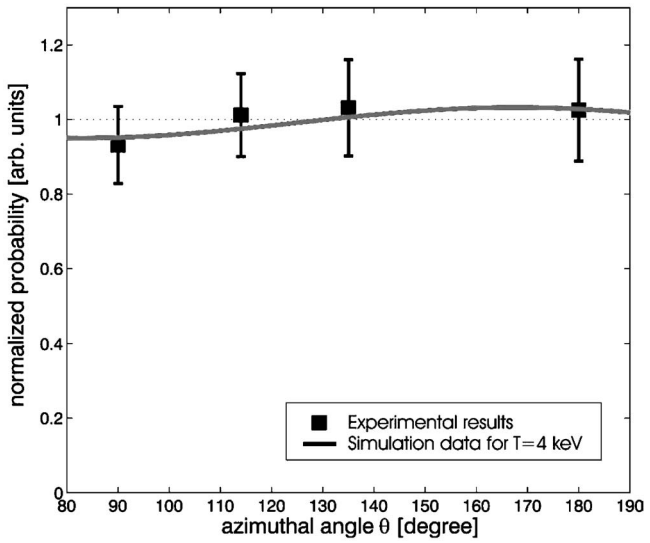

FIG. 3. Azimuthal neutron scan in D_2 and comparison with data from a particle simulation. The error bars indicate the standard deviation obtained from the standard deviation of the signal areas.

IV. INTERPRETATION OF RESULTS

As shown in the polarization scan data (Fig. 4), the neutron emission is essentially independent of the polarization. The immediate conclusion is that there is no prevailing polarization for any of the detector positions. Moreover, this polarization measurement can be taken as an indication for the cylindrical symmetry in the plasma filament since all other physical parameters can be assumed to be constant over its initial diameter of less than 100 μm. From Fig. 5 we can see that the neutron emission is anisotropic in the azimuthal plane for CD_4 clusters. Similar behavior may be evident in D_2 clusters (Fig. 3), though the size of the error bars and the small magnitude of the effect preclude a definitive answer in this case. The forward or backward peaking of the neutron emission is clearer in CD_4 clusters; the probability for a neutron emission varies over different azimuthal angles by as much as 43% in CD_4.

We believe that there are two major contributions to the observed anisotropy: on the one hand, the cylindrical geometry of the plasma filament and, on the other hand, the one-

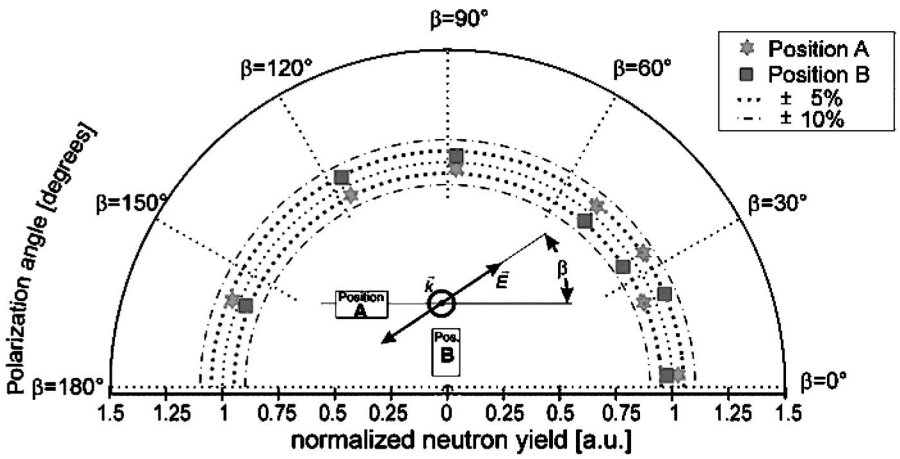

FIG. 4. Measured neutron emission from a CD_4 plasma in the plane perpendicular to the laser propagation as a function of angle with respect to the laser polarization.

sided irradiation of the cluster plume that results in preferential deposition of energy on one side of the plume. Fusion collisions have a slightly higher differential cross section for emission of a neutron along the axes of the ion collision [22], even at the modest energies of the ions driving the fusion in our plasma (the hot tail of ions with energy 30–1000 keV). Because the filament is a long cigar-shaped filament, there is a higher number of collisions between ions emitted from the exploding clusters along the cylinder axis. In addition, beam-target collisions of the emitted ions colliding with atoms in the surrounding gas will occur. A greater number of collisions will occur with ions emitted in the direction of the filament because there is a greater path of gas for the ions to traverse in this direction.

To ascertain the magnitude of these effects, we have examined the probability of fusion between two hot ions in the filament and beam-target fusion between a hot ion and a cold nucleus in the surrounding gas. First, we assume that the ion energy spectrum is Maxwellian. This is a good assumption based on our previous measurements of the ion spectrum from exploding deuterium clusters [23]. We have found that a Maxwellian-like energy distribution results in our plasmas as a result of the convolution of the Coulomb explosion spectrum from a single cluster and the log-normal size distribution of clusters in our gas jet. To assess the relative contributions of beam-target fusion and fusion between hot ions in the filament, we can examine the appropriate averaged cross section. Beam-target fusion per fast ion will have a probability proportional to the fusion cross section weighted by the ion energy distribution

$$\langle \sigma_T \rangle_{BT} = \int_0^\infty f_T(v)\sigma\left(\frac{1}{2}mv^2\right)dv, \tag{1}$$

where $1/2\ mv^2$ is the energy of the collision, and the Maxwell distribution $f_T(v)dv$ provides the probability to find an ion with a velocity within the interval $[v,v+dv]$. Fusion

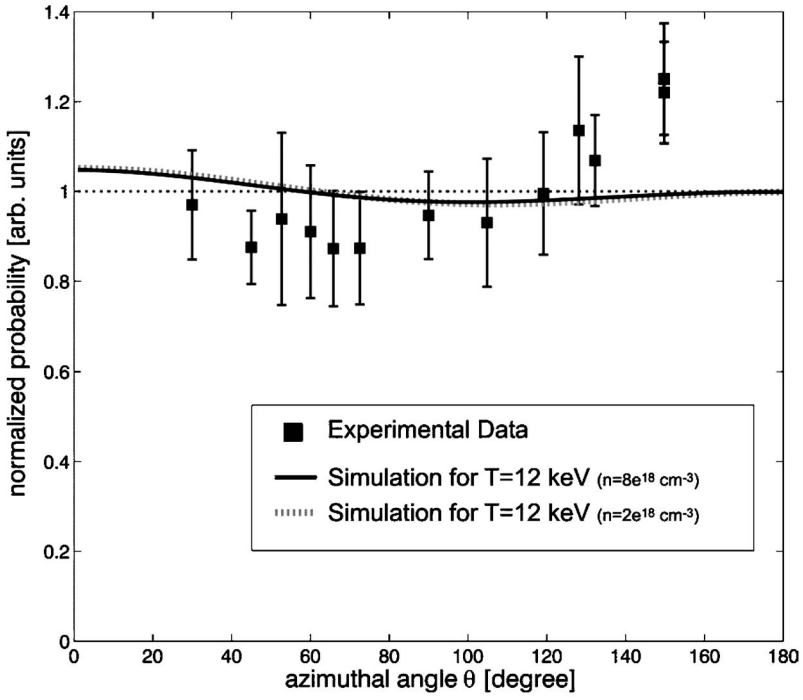

FIG. 5. Azimuthal neutron scan in CD_4 and comparison with data from a particle simulation.

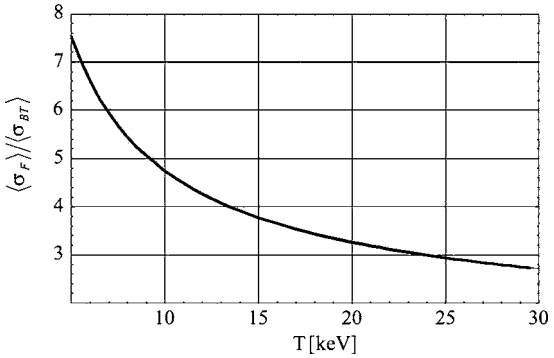

FIG. 6. Ratio of the average cross section for ion-ion interaction in the filament (subscript F) and for interactions in the beam target (subscript BT).

probability between two hot ions in the filament will be proportional to this averaged cross section,

$$\langle \sigma_T \rangle_F = \frac{1}{2\pi} \int_0^\infty \int_0^\infty \int_0^{2\pi} f_T(v_1) f_T(v_2) \sigma \left[\frac{1}{2} m (v_1^2 + v_2^2 - 2 v_1 v_2 \cos \alpha) \right] d\alpha \, dv_1 \, dv_2, \tag{2}$$

where α denotes the angle between the directions of motion of both particles, v_1 is the velocity of the first particle, and v_2 the velocity of the second particle. For each temperature we computed the ratio $\langle \sigma_T \rangle_F / \langle \sigma_T \rangle_{BT}$ by fitting cross-section data from Ref. [24] and by integrating numerically. Figure 6 plots the ratio of these two cross sections as a function of the effective temperature of the plasma. Our previous measurements suggest an effective temperature in the deuterium cluster plasmas of $\approx 5-10$ keV [23]. Figure 6 indicates that at this temperature each ion has a five times higher probability of fusion per unit length of gas traversed in the hot filament than in the surrounding cold gas. However, the ion traverses a path in the surrounding gas which is roughly ten times as long as the average path in the filament. So we expect that fusion between ions in the filament and from beam-target fusion to give a roughly comparable contribution to the observed fusion yield.

As a consequence of this simple analysis, we believe that both reasons offered above (filament shape and asymmetry in deposited energy in the gas plume) may contribute to the anisotropy of neutrons observed in our experiment. To analyze this assertion more quantitatively, we have calculated fusion angular distributions using a Monte Carlo particle code. This simulation is based upon the idealized model of a cylindrically shaped hot plasma that is surrounded by a spherical cloud of cold gas. It was assumed that all ions are initially situated at random spatial positions in the filament and start propagating in random directions at velocities obeying a Maxwellian distribution. For each ion the minimal distances along its trajectory to all other ions and all nuclei in the ambient plume were calculated. The energy depletion per unit length for a proton is on the order of 23 keV/cm at typical densities in a gas jet plume ($\approx 5 \times 10^{18}$ cm^{-3}) [25]. For the simulation we assume that very hot ions (which are the ones that drive the nuclear fusion) from the filament can traverse the hot plasma and surrounding cold gas, which extends over a few millimeters, with no or little modification to their energy.

In the simulation, if one or more particles were closer than $R=0.45$ nm, they were regarded as a collision. This is equivalent to the assumption that each particle in our simulation does not represent an isolated ion but a disc of multiple ions with 0.45 nm radius. This synthetic cross section is much bigger than the actual fusion cross section, but we can assume that the paths of the ions through the area given by πR^2 are going to be uniformly distributed. Then the probability to fuse is proportional to the particular cross section at the energy which is associated with the relative motion of both "superparticles." The total probability for a collision leading to a fusion event was then obtained for every direction by summing all fusion probabilities in each given bin of the solid angle. Finally, the azimuthal neutron distribution $f(\theta)$ was calculated in the plane of $\phi = 0° \pm 5°$ by integrating the contribution of the differential cross section from each set of collisions.

The simulation was run for varying numbers of hot ions in the filament and cold nuclei in the surrounding beam target at different temperatures, different density distributions, and different aspect ratios. While the absolute temperature and also the spatial temperature profile in the filament were found to have only a weak influence on the resulting angular emission pattern, the geometry of the beamtarget, its spatial density distribution, and the aspect ratio of the filament have a much more pronounced effect on the extent of the anisotropy. More specifically for the beam target contribution, the number of nuclei, i.e., the abundance of potential collision partners along different directions of motion (as seen from the filament), determines the angular fusion probability and hence the neutron emission probability. For various sets of parameters, we found no evidence in our simulation for any dependence of the neutron emission pattern on the total density as long as the same gas jet geometry was assumed. This is to be expected since the probabilities for an ion to fuse while in the filament and while in the beam target both scale linearly with density. Therefore the relative contribution of these two processes should not change with overall density.

We find numerically that the fusion observed does indeed rise approximately equally for collisions between two hot ions in the filament and collisions between a hot ion and a cold nucleus in the surrounding gas. Our simulation does predict a slight peaking of the neutron emission on the axes along the laser propagation direction. The results of our simulations are shown, overlaid on the azimuthal neutron emission data of Fig. 3 and Fig. 5. In both cases, in D_2 clusters and in CD_4 clusters, the simulation predicts a slight peaking of the fusion neutrons in the forward and backward direction.

In the comparison with D_2 cluster data in Fig. 3, we assumed a filament with an initial diameter of 100 μm and a length of 1 mm. The filament was placed in the leading edge of a bath of cold gas that was 1.9 mm in diameter. In other words, the filament penetrated only halfway into the gas. This is consistent with our previous imaging of the plasma filament [26]. The initial ion temperature of ions in the fila-

ment was 4 keV and the average deuterium ion density was the equivalent of 1×10^{19} cm^{-3}. Fusion from ions in the filament accounts for about 20% of the total fusion yield. As discussed above, the slight peaking evident in the simulation arises from the fact that there are a greater number of fusion events from particles emitted in the forward direction because they have a greater path of hot gas and surrounding cold gas to traverse before exiting the deuterium gas. The slight peaking of the differential cross section in the forward and backward directions is sufficient to give rise to the slight anisotropy seen in the simulation. Though, as mentioned previously, these data exhibit error bars larger than the observed anisotropy, the simulation is consistent with the modest anisotropy observed in the experiment.

In the simulation of the CD_4 data presented in Fig. 5, we observe a more pronounced peaking of the neutrons in the forward and backward directions, a trend also consistent with the measurements. We assumed an initial ion temperature of 12 keV (consistent with measurements of ion energies in deuterated methane clusters) and our estimated average deuterium ion density of 8×10^{18} cm^{-3}. The background gas density profile is similar to that which we measure in the plume (with a flat profile in the center of the plume and a $1/r$ fall off in density toward the edges). A simulation performed with a lower deuterium ion density of 2×10^{18} cm^{-3} (molecular density of 5×10^{17} cm^{-3}) exhibits an almost identical angular distribution. The simulated result shows qualitatively the same behavior as the data, though the experiment seems to show an even more pronounced peaking of neutrons along the laser propagation axis than the simulation. This result is somewhat puzzling but may be a result of an inaccurate representation of the plume around the filament in the simulation. Nonetheless, the simulation confirms the importance of the two geometric effects that we have described.

Finally, we note that the neutron angular distribution we measure differs from the results reported by Grillon *et al.* [10], who saw an almost 40% increase of the neutron yield at 54° from the forward direction. We find this surprising, given the similar experimental setup and operating conditions of the gas jet. In that experiment, the gas density was assumed to be lower than here although our analysis suggests that this should not affect the angular distribution. The discrepancy perhaps could arise from differences in the spatial density profile of the gas plume or from the exact details of the laser energy deposition.

V. CONCLUSIONS

In conclusion, we have measured the angular distribution of neutrons emitted from fusion of deuterium ions from laser driven explosions of D_2 and CD_4 clusters. We find that there is no dependence of the neutron emission with respect to the angle between the emission and the laser electric field axis. We do, however, find that there is a slight peaking of the neutron emission along the axis defined by the laser propagation direction. The angular profile we observe is a consequence of the geometry of the gas plume and hot filament from which the fusion arises. The qualitative aspects of our observed fusion anisotropy can be explained with a simple Monte Carlo particle model.

ACKNOWLEDGMENTS

We would like to acknowledge many fruitful discussions with Alexander Maltsev and Boris Breizman about the simulation and data analysis. This work was supported by the U.S. Department of Energy Office of Basic Energy Sciences and by the National Nuclear Security Administration under Cooperative Agreement No. DE-FC52-03NA00156.

[1] A. McPherson, B. D. Thompson, A. B. Borisov, K. Boyer, and C. K. Rhodes, Nature (London) **370**, 631 (1994).
[2] H. Wabnitz, L. Bittner, A. R. B. De Castro, R. Döhrmann, P. Gürtler, T. Laarmann, W. Laasch, J. Schultz, A. Swiderski, K. Von Haeften, T. Möller, B. Faatz, A. Fateev, J. Feldhaus, C. Gerth, U. Hahn, E. Saldin, E. Schneidmiller, K. Sytchev, K. Tiedtke, R. Treusch, and M. Yurkov, Nature (London) **420**, 482 (2002).
[3] T. Ditmire, J. W. G. Tisch, E. Springate, M. B. Mason, N. Hay, R. A. Smith, J. Marangos, and M. H. R. Hutchinson, Nature (London) **386**, 54 (1997).
[4] I. Last and J. Jortner, Phys. Rev. Lett. **87**, 033401 (2001).
[5] I. Last and J. Jortner, J. Phys. Chem. A **106**, 10877 (2002).
[6] B. N. Breizman and A. V. Arefiev, Plasma Phys. Rep. **29**, 593 (2003).
[7] T. Ditmire, J. Zweiback, V. P. Yanovsky, T. E. Cowan, G. Hays, and K. B. Wharton, Nature (London) **398**, 489 (1999).
[8] J. Zweiback, R. A. Smith, T. E. Cowan, G. Hays, K. B. Wharton, V. P. Yanovsky, and T. Ditmire, Phys. Rev. Lett. **84**, 2634 (2000).
[9] J. Zweiback, T. E. Cowan, R. A. Smith, J. H. Hartley, R. Howell, C. A. Steinke, G. Hays, K. B. Wharton, J. K. Crane, and T. Ditmire, Phys. Rev. Lett. **85**, 3640 (2000).
[10] G. Grillon, Ph. Balcou, J.-P. Chambaret, D. Hulin, J. Martino, S. Moustaizis, L. Notebaert, M. Pittman, Th. Pussieux, A. Rousse, J.-Ph. Rousseau, S. Sebban, O. Sublemontier, and M. Schmidt, Phys. Rev. Lett. **89**, 065005 (2002).
[11] G. Pretzler, A. Saemann, A. Pukhov, D. Rudolph, T. Schätz, U. Schramm, P. Thirolf, D. Habs, K. Eidmann, G. D. Tsakiris, J. Meyer-ter-Vehn, and K. J. Witte, Phys. Rev. E **58**, 1165 (1998).
[12] L. Disdier, J-P. Garçonnet, G. Malka, and J-L. Miquel, Phys. Rev. Lett. **82**, 1454 (1999).
[13] D. Hilscher, O. Berndt, M. Enke, U. Jahnke, P. V. Nickles, H. Ruhl, and W. Sandner, Phys. Rev. E **64**, 016414 (2001).
[14] P. Norreys, A. P. Fews, F. N. Beg, A. R. Bell, A. E. Dangor, P. Lee, M. B. Nelson, H. Schmidt, M. Tatarakis, and M. D. Cable, Plasma Phys. Controlled Fusion **40**, 175 (1998).
[15] N. Izumi, Y. Sentoku, H. Habara, K. Takahashi, F. Ohtani, T. Sonomoto, R. Kodama, T. Norimatsu, H. Fujita, Y. Kitagawa, K. Mima, K. A. Tanaka, and T. Yamanaka, Phys. Rev. E **65**, 036413 (2002).

[16] C. Toupin, E. Lefebvre, and G. Bonnaud, Phys. Plasmas **8**, 1011 (2001).

[17] V. S. Belyaev, V. I. Vinogradov, A. S. Kurilov, A. P. Matafonov, V. P. Andrianov, G. N. Ignat'ev, A. Ya. Faenov, T. A. Pikuz, I. Yu. Skobelev, A. I. Magunov, S. A. Pikuz, Jr., and B. Yu. Sharkov, JETP **98**, 1133 (2004).

[18] S. Fritzler, Z. Najmudin, V. Malka, K. Krushelnick, C. Marle, B. Walton, M. S. Wei, R. J. Clarke, and A. E. Dangor, Phys. Rev. Lett. **89**, 165004 (2002).

[19] S. Karsch, S. Düsterer, H. Schwoerer, F. Ewald, D. Habs, M. Hegelich, G. Pretzler, A. Pukhov, K. Witte, and R. Sauerbrey, Phys. Rev. Lett. **91**, 015001 (2003).

[20] M. Schnürer, D. Hilscher, U. Jahnke, S. Ter-Avetisyan, S. Busch, M. Kalachnikov, H. Stiel, P. V. Nickles, and W. Sandner, Phys. Rev. E **70**, 056401 (2004).

[21] S. Ter-Avetisyan, M. Schnürer, D. Hilscher, U. Jahnke, S. Busch, P. V. Nickles, and W. Sandner, Phys. Plasmas **12**, 012702 (2005).

[22] Ronald E. Brown and Nelson Jarmie, Phys. Rev. C **41**, 1391 (1990).

[23] K. W. Madison, P. K. Patel, D. Price, A. Edens, M. Allen, T. E. Cowan, J. Zweiback, and T. Ditmire, Phys. Plasmas **11**, 270 (2004).

[24] J. D. Huba, *NRL Plasma Formulary*, (Naval Research Laboratory, Washington, D.C., 2000), p. 44.

[25] The stopping power was obtained with the PSTAR code by M. J. Berger, National Institute of Standards and Technology, Physics Laboratory, Ionizing Radiation Division, http://physics.nist.gov/PhysRefData/Star/Text/contents.html

[26] J. Zweiback and T. Ditmire, Phys. Plasmas **8**, 4545 (2001).